Coupling geochemical tracers and pesticides to determine recharge origins of a shallow alluvial aquifer: Case study of the Vistrenque hydrogeosystem (SE France)

Lara Sassine, Mahmoud Khaska, Sophie Ressouche, Roland Simler, Joël Lancelot, Patrick Verdoux, Corinne Le Gal La Salle

Coupling geochemical tracers and pesticides to determine recharge origins of a shallow alluvial aquifer: Case study of the Vistrenque hydrogeosystem (SE France)

Lara Sassine [a,b,*], Mahmoud Khaska [a], Sophie Ressouche [c], Roland Simler [d], Joël Lancelot [a], Patrick Verdoux [a], Corinne Le Gal La Salle [a,b]

[a] Univ. Nimes, EA 7352 CHROME, rue du Dr Georges Salan, 30021 Nimes, France
[b] CEREGE, UM34, University of Aix-Marseille, 13545 Aix-en-Provence Cedex 4, France
[c] Joint Venture of the Vistrenque and Costières Groundwaters, 30600 Vauvert, France
[d] Laboratory of Hydrogeology, EMMAH, UMR 11144, University of Avignon, 84000 Avignon, France

A B S T R A C T

The objective of this study is to identify the origin of groundwater in a shallow alluvial aquifer, using a multi-tracer approach including $\delta^{18}O$, $\delta^{2}H$, major elements and $^{87}Sr/^{86}Sr$. In addition, triazines are used as a tracer of water draining agricultural areas.

Four potential recharge sources are evidenced in the alluvial groundwater: rainfall, karst water from adjacent aquifer, imported Rhône river water and local stream water.

Strontium isotopes are used to highlight the adjacent karst water input ($Sr = 6.4–17.6$ µmol L^{-1}; $^{87}Sr/^{86}Sr = 0.7076–0.7078$) showing a contrasting signature with the pristine alluvial groundwater ($Sr = 3.4$ µmol L^{-1}; $^{87}Sr/^{86}Sr = 0.7088–0.7092$). Lateral karst recharge is observed, with high proportions reaching 100%, all along the North Western border of the aquifer. This lateral recharge implies a dilution in triazines content of the Vistrenque groundwater as the karst area is not used for agriculture.

Oxygen-18 and deuterium signatures of local rainwater ($\delta^{2}H = -43.5‰$) and imported Rhône River water ($\delta^{2}H = -72.5‰$) differ significantly which allows to quantify the influence of imported water on the alluvial groundwater. Such influence is observed only locally in this study. Contribution of local stream water, influenced by wastewater treatment plant effluents, is also locally detected in the alluvial aquifer, using Cl, K, and Na contents.

High triazines, NO_3, and Cl concentrations underline the vulnerability of this shallow alluvial aquifer to surface contaminations. Finally, the results of this environmental multi-tracer approach are statistically supported by principal component analyses.

1. Introduction

Alluvial aquifers are the largest groundwater reservoir used for public water supply in European countries (Ray, 2002). These reservoirs are quite vulnerable to anthropogenic contaminations such as fertilizers and pesticides. In addition, the occurrence of emerging organic contaminants (EOCs) in groundwater bodies arises (Fram and Belitz, 2011; Lapworth et al., 2012; Stuart et al., 2012). In order to protect water resources, the EU Water Framework Directive (WFD 2000/60/EC) and its daughter Groundwater Directive (2006/118/EC) established environmental objectives to achieve a "good status" in 2015. As alluvial aquifers may be recharged not only from rain, but also from other sources such as surface water or adjacent reservoirs, the hydrological functioning of this type of aquifers and particularly the origin of groundwater must be defined, to better prevent, assess or remediate the EOC and pesticide contaminations.

The aim of this study is to characterize the different water bodies contributing to a shallow alluvial aquifer recharge using a multi-tracers approach based on chemical elements and isotope tracers such as $^{87}Sr/^{86}Sr$, $\delta^{18}O$, and $\delta^{2}H$. These geochemical tracers are coupled to triazines, used as a tracer of groundwater originating from hydrosystems with agricultural land uses.

Many studies used chemical and/or isotopic approaches to characterize the origin of groundwater in alluvial aquifers but very few associated them to the understanding of organic contaminant

* Corresponding author at: Laboratory of Environmental Isotopes Geochemistry, University of Nîmes, Georges Besse Scientific Park, 150 Georges Besse Street, 30035 Nîmes Cedex 1, France. Tel.: +33 466709979.
E-mail address: lara.sassine@unimes.fr (L. Sassine).

sources in groundwater bodies (Cary et al., 2013; Osenbrück et al., 2007).

In previous studies, stable isotopes, generally conservative in shallow groundwater systems, have been used to determine the contribution of different recharge sources to groundwater (Dogramaci and Herczeg, 2002; Mohammed et al., 2014; Négrel et al., 2004; Rains and Mount, 2002; Thiros and Manning, 2004; Williams, 1997), the relationship between groundwater and rivers (Christophersen et al., 1990; Gourcy and Brenot, 2011; Hooper, 2001; Hooper et al., 1990; Mas-Pla et al., 2012), and to evidence imported water, generally diverted from higher elevations in canals and used for irrigation and/or public water supply (De Montety et al., 2008; Moran and Hudson, 1990; Stalker et al., 2010; Williams and Rodoni, 1997). Hence, $\delta^{18}O$ and $\delta^{2}H$ can be used to quantify the contribution of imported water either by excess irrigation, distribution canal loss, artificial recharge, leakage processes from the underground water distribution system, unsealed septic tanks, or wastewater treatment plants (WWTP) inputs.

Similarly and despite its geochemical reactivity, strontium isotopes prove to be a good tracer to differentiate water bodies issued from aquifers with different geological formations (Aberg, 1995; Dogramaci and Herczeg, 2002; Frost and Toner, 2004; Négrel et al., 2004; Voerkelius et al., 2010). Though, the $^{87}Sr/^{86}Sr$ composition may be influenced by exogenous sources like fertilizers that show large variations in isotopic compositions and concentrations (Böhlke and Horan, 2000; Négrel et al., 2004; Pierson-Wickmann et al., 2009; Vitòria et al., 2004). Owing to its conservative behavior in groundwater systems, Cl can be coupled to Sr to better understand the prevailing processes (Gosselin et al., 2004). Major elements, such as Na, K, and Cl, are essentially used to trace anthropogenic contaminations, such as WWTP or landfill contributions (Andersen et al., 2004). Finally, due to their high frequencies of detection in groundwater bodies (Kolpin et al., 2004; Loos et al., 2010) and their persistence in the underground system (Baran et al., 2007; Lapworth and Gooddy, 2006; Loos et al., 2010; Steele et al., 2008; Tesoriero et al., 2007; Vonberg et al., 2014), triazines (atrazine, simazine and their degradation products deethylatrazine "DEA" and deisopropylatrazine "DIA"), which are selective herbicides used in agricultural crops, can characterize water infiltrating in agricultural areas where they were frequently used prior to their prohibition in 2003.

The study site, the Vistrenque alluvial aquifer along with the Costières aquifer, has a high socio-economic importance, since approximately 14 million m^3/a are used for public water supply over 43 townships, corresponding to 130,000 inhabitants in the south of the Gard department (Southern France) (Fig. 1a), 4–9 million m^3/a are abstracted for agricultural uses, 3 million m^3/a for

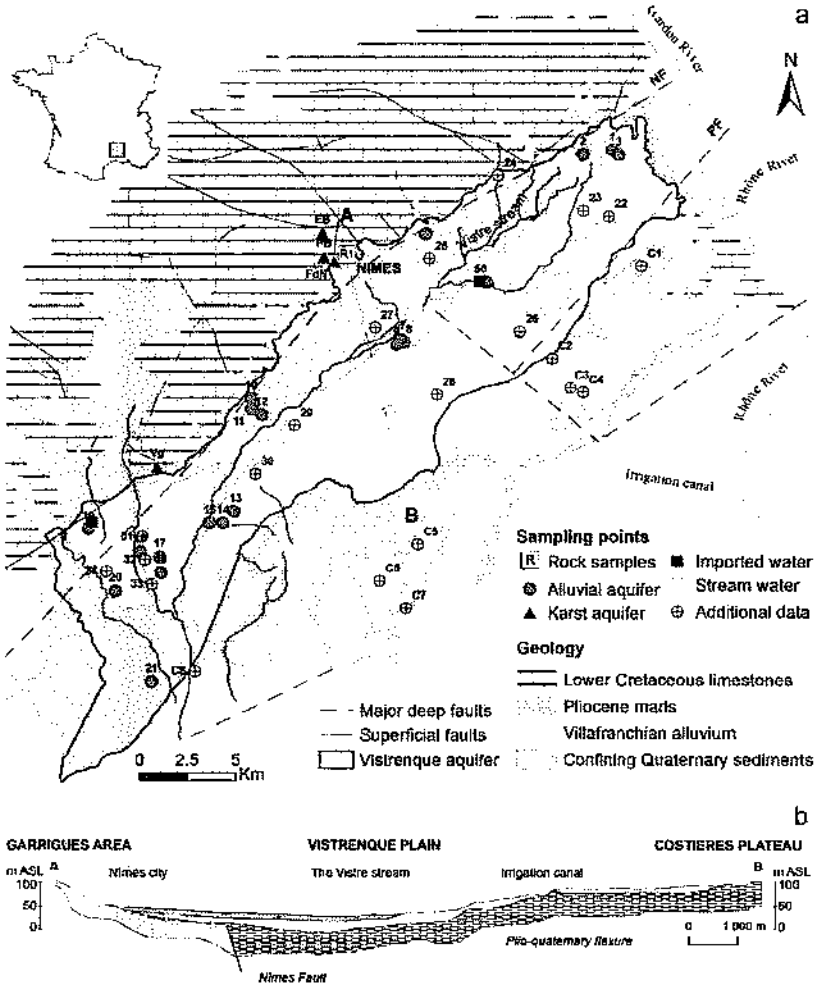

Fig. 1. (a): Sketched geological map of the study site, showing local geology, sampling point locations and an A–B cross section. NF: Nîmes Fault, PF: Pujaut Fault; (b): A–B simplified cross section from the Garrigues area to the Costières plateau (modified from Poul et al., 1975).

industrial uses and 2–3 million m^3/a for personal supply (SMNVC, 2010). The prevalent land use over the Vistrenque plain is agriculture, which induces nitrates and pesticides diffuse groundwater pollutions, firstly evidenced by drinking water quality control.

2. Site of study

2.1. Geological settings

The Vistrenque aquifer is a 325 km^2 shallow alluvial aquifer mostly unconfined while locally confined with loess and silts deposits of recent Quaternary age, at the right bank of the Vistre stream (Fig. 1a). At a local scale, it is bordered on the North West by the Garrigues area, named relatively to the occupying Mediterranean vegetation and hosting a karst aquifer in the lower Cretaceous limestones. On the South East, it is bordered by the Costières Plateau, hosting two distinct alluvial aquifers in Villafranchian alluvium. The Vistrenque aquifer is included in a NE–SW graben structure, which is approximately 10 km wide and 30 km long (Fig. 1a and b).

The regional geological basement is formed of lower Cretaceous (136–130 Ma) limestones, folded and fractured during the Pyrenean orogeny phase over the Eocene (Benedicto et al., 1996; Séranne et al., 1995). In this period, the Fault of Nîmes has set up as a normal fault, differentiating a NW and a lowered SE limestone compartments. During Lower Pliocene (Plaisancian stage), marine clays and marls, constituting the confining bed of the Vistrenque aquifer, were deposited on the SE Cretaceous compartment. This 200–700 m thick impermeable layer was overlain by Quaternary fluvial sediments, including Villafranchian alluvium, which constitutes the reservoir of the Vistrenque and the Costières aquifers (Poul et al., 1975). This alluvial formation includes a high proportion of gravels and pebbles, mainly constituted of quartzites, milky quartz, and limestones, and in lower proportion, granites, gneiss, basalts and sandstones (Ménillet and Paloc, 1973) in a sandy carbonated matrix. The alluvium thickness varies from 5 m in the NE to 20–30 m in the SW. During the post-Villafranchian period, the NE–SW Plio-Quaternary flexure of Vauvert (Fig. 1b) has caused the raise of the Costières Plateau (Poul et al., 1975). A layer of loess and silt deposits of recent Quaternary age covers the Vistrenque alluvium along the limestones boundary, partially confining the aquifer at this location.

2.2. Hydrological and hydrogeological settings

The average annual precipitation over the last 20 years is about 700 mm/year at Nîmes–Courbessac weather station (http://publitheque.meteo.fr/), located in the Vistrenque plain, and about 800 mm over the karst area (Maréchal et al., 2004).

2.2.1. The Vistrenque plain

In the Vistrenque alluvial aquifer, the groundwater flows in a NE–SW general direction. The permeability of the Villafranchian alluvium varies within the aquifer between 3×10^{-3} and 10^{-4} m s^{-1} (Poul et al., 1975). The groundwater level varies between 2 and 6 m below ground surface, during the annual hydrological cycle.

The Vistrenque plain is crossed by a local stream, The Vistre, along 45 km (Fig. 1a). The Vistre originates from the confluence of several branches, some draining the Garrigues area and others the Vistrenque aquifer, with a hydrographic catchment of 586 km^2. The stream bed has been extensively modified first to accommodate water mills, and then straighten and deepened to facilitate drainage.

Currently the relationship between the Vistre stream and the Vistrenque groundwater is not very well defined. Burgeap and Sarl Gren (2006) showed that the stream and the groundwater are hydraulically disconnected on the first 26 km (Fig. 1a), due to a thick siltstones layer separating the stream water from the groundwater table. On the next 3 km, the stream and the groundwater are hydraulically connected. On the remaining part of the stream, the connection between stream water and groundwater is weak as the aquifer becomes confined.

Imported "Rhône River" water is brought to the Vistrenque plain via canals network, used for irrigation and water supply. In addition, the city of Nîmes is supplied by the groundwater abstracted from one of the Rhône alluvial aquifers, the Comps aquifer, fed by both the Rhône and the Gardon river waters.

2.2.2. The adjacent karst limestones aquifer

The karst aquifer includes 2 geological systems; one in the northern and the north eastern area, the Barremian system, and a second one in the southern and the south western area, the Hauterivian system which host the Fountain of Nîmes (FdN) spring system (Fabre, 1997) (Fig. 1a). The hydrogeology of the FdN spring was essentially discussed in karst flash flood studies (Maréchal et al., 2008).

The relationship between the Vistrenque alluvial aquifer and the adjacent karst limestone aquifer was previously investigated on the basis of pumping tests, flow analyses and geochemical analyses using Sr isotopes, on 2 sites near the city of Nîmes (Dorfliger et al., 1999; Fabre, 1988; Michel and François, 1995).

3. Sampling and analytical methods

3.1. Sampling procedure

Groundwater (GW) samples were collected from 21 boreholes on the Vistrenque plain and 4 boreholes on the karst area, listed in Table 1S (Supplementary data). Four sampling campaigns were carried out, two at the end of the dry season, in September 2011 and September 2012, and two toward the end of the wet season, in March 2012 and July 2013. Data of September 2012 campaign are not presented. In order to ascertain the influence of some water bodies on the Vistrenque groundwater, 13 other boreholes on the Vistrenque plain (numbered from 22 to 34 in Fig. 1a) and 8 boreholes on the Costières Plateau (C1–C8, Fig. 1a) were sampled in an additional campaign that was carried out in December 2013 (Table 2S; Supplementary data).

Before collecting water samples, private wells were purged, with a SDEC pump (5 L min^{-1}), until stabilization of physico-chemical parameters of groundwater. The physico-chemical parameters (temperature, pH, oxydo-reduction potential, specific conductance at 25 °C and dissolved oxygen) were measured *in situ* in a flow through cell to prevent contact with the atmosphere using a WTW multi 340i.

Alkalinity was determined in the field by volumetric titration (1.6 N H_2SO_4) using a Hach Lange titrator. Considering pH conditions, alkalinity was reported as HCO_3 concentrations.

Water was filtered online with 0.45 µm ceramic filter and collected in pre-cleaned 60 mL polyethylene bottles for anions, cations, Sr concentration and Sr isotopic composition analyses. For cations and Sr analyses, samples were acidified with ultrapure HNO_3 to pH ≈ 3. Raw water was collected in 10 mL glass bottles avoiding air bubbles for $\delta^{18}O$ and $\delta^{2}H$ analyses. Groundwater to be analyzed for triazines was collected in pre-cleaned and baked, 1 L amber glass bottles, with Teflon lined caps. Samples were filtered through 0.7 µm glass fiber filters in laboratory then shipped on ice to Eurofins accredited laboratory.

Rock samples, to be analyzed for Sr signature, were leached according to the conditions listed in Table 3S (Supplementary

data), considered after Khaska et al. (2013). All leachates are analyzed for Sr isotopic composition (Table 3S). In addition, the easily leachable fraction of Plaisancian marls (R2a) is analyzed for Cl and Sr concentrations in order to determine its Cl/Sr ratio.

3.2. Analytical method

3.2.1. Major and trace elements

Major elements (Ca, Mg, Na, K, NH_4, Cl, SO_4, and NO_3) and bromide (Br) analyses were carried out on ion chromatography with 5% and 8% uncertainties respectively at the Laboratory of Hydrogeology of Avignon University. Sr concentrations were analyzed by ICPMS at the Laboratory of Hydrology and Geochemistry of Strasbourg University. Uncertainty is of 3%.

3.2.2. Strontium isotope analyses

Sr was purified in clean room by cationic extraction chromatography using precleaned 100 µL Sr Spec-resin from Eichrom according to the method developed by Pin et al. (2003). Samples were loaded on previously outgassed single Re filaments between 2 layers of Ta_2O_5–H_3PO_4–HF activator solution. The filament was brought to red heat to remove excess acid.

Isotope ratios were measured by thermal ionization mass spectrometry using a nine-collector Finnigan Triton TI equipped with a 21 samples turret. The resulting values were normalized to $^{88}Sr/^{86}Sr = 8.375209$ to correct for mass bias and were corrected for eventual isobaric interferences for ^{87}Rb by using the natural $^{87}Rb/^{85}Rb$ ratio = 0.385714 and measuring ^{85}Rb. Sr concentrations of blank samples were of 0.33 ng, so corrections for blanks were not necessary. $^{87}Sr/^{86}Sr$ ratios of individual analyses gave 2σ uncertainties less than 9×10^{-6}. Replicates of the NBS 987 standard, during the period of analysis, gave an average $^{87}Sr/^{86}Sr$ ratio of $0.71025 \pm 1.3 \times 10^{-5}$ ($n = 42$; 2σ). In order to monitor the reproducibility of the overall process, one of the samples was analyzed on 3 separate runs, the overall standard deviation was 4×10^{-5} ($n = 3$; 2σ).

3.2.3. Water isotope analyses

Oxygen and hydrogen isotopes compositions were determined by cavity ring down spectrometry using a Picarro L 2130i according to the analytical scheme recommended by the IAEA (Penna et al., 2010). $\delta^{18}O$ and $\delta^{2}H$ are reported in per mil (‰) relative to the V-SMOW (Vienna Standard Mean Ocean Water) reference material, and calibrated with the internal standards from IDES Laboratory (Interactions and Dynamic of Surface Environments) of Paris-Sud University. The average uncertainties for $\delta^{18}O$ and $\delta^{2}H$ on individual analyses were respectively in the order of 0.1‰ and 0.4‰ ($n = 6$, 2σ). Replicates of deionised water ($n = 90$; 2σ) gave uncertainties for $\delta^{18}O$ and $\delta^{2}H$ of the same order of magnitude.

All isotopic analyses and Sr purification were carried out at the Laboratory of Environmental Isotope Geochemistry of Nîmes University.

3.2.4. Pesticides analyses

Analyses of triazines (atrazine, simazine, DEA, and DIA) in water samples were performed after solid phase extraction by liquid chromatography with tandem mass spectrometry (SPE-LC/MSMS) at the accredited Eurofins Laboratory (Montpellier, France). The limit of quantification (LQ) is of 5 ng L^{-1} for each compound and the measurement uncertainty is estimated to be around 20–50%.

3.3. Literature data

The chemical and isotopic ($\delta^{18}O$, $\delta^{2}H$) compositions of rainwater on the study area are derived from Ladouche et al. (2009) (1998–2002) and from GIS laboratory rain gauge data (2010–2013; Table 1S). Bromide concentrations in rainwater from Ladouche et al. (2009) were reconstructed on the basis of marine fractions. Precipitation data are reported as volume weighted annual average (VWA) for both references.

The Costières alluvial groundwater chemical composition is acquired from ADES database (http://www.eaufrance.ades.fr/) on 5 municipal wells. Average compositions are computed when multiple analyses are available.

The chemical and Sr isotopic compositions of the pristine karst water are reported from Maréchal et al. (2005). The naming system of karst wells sampled during this study are conserved as in Maréchal et al. (2005).

The annual average chemical composition of the imported canal water (2011–2013) is acquired from the managing company (http://www.brl.fr/; Table 1S).

4. Results

4.1. Physico-chemical parameters

The average temperature of the Vistrenque alluvial groundwater is around 16 °C. Most of the total dissolved solids (TDS) of all water bodies fall within the freshwater range (275–750 mg L^{-1}) (Table 1S). TDS of imported water falls within the lower values of that range (275–350 mg L^{-1}), that of karst and Costières groundwater in the middle and, finally TDS of stream water falls in the upper range (640–730 mg L^{-1}). Vistrenque groundwater TDS values cover the full range of the above cited water bodies TDS. Locally, the TDS reaches the highest levels (700–1056 mg L^{-1}) at boreholes located in environments exposed to anthropogenic contaminations, such as a food processing effluents (FPE) spreading field (sites 13 and 14), or, an area, at the South of the aquifer, known for intensive market garden activity implying N-fertilizers usage, and hydroponic cultures using nutrient solutions rich in N, K, Ca and Mg (sites 16, 17, 18, 21).

Both Vistrenque and karst groundwater bodies are slightly acidic to neutral (pH ranging from 6.2 to 7.6) unlike more basic surface water that show a pH variation between 7.1 and 8.5 that may be due to degassing of groundwater discharging into the stream. The dissolved oxygen (DO) content in the Vistrenque groundwater normally ranges between 4 and 8.5 mg L^{-1}; lowest values (0.1–2 mg L^{-1}), characterizing suboxic environments, are observed on sites located near stream water bodies (sites 5, 6, 15), in the FPE spreading field (sites 13, 14) or at the outlet area of the aquifer (site 21). Karst water DO falls within the lowest range (1.5–5.2 mg L^{-1}) while surface water DO falls within the highest range (4.1–9.8 mg L^{-1}), close to the equilibrium with the atmospheric oxygen content (considered of 10 mg L^{-1} during the calibration).

Beside the sites located in environments exposed to anthropogenic contaminations (sites 13, 14, 16, and 21), the groundwater physico-chemical parameters as well as major ion concentrations (Section 4.3) remain fairly stable (within 10%) over the sampling campaigns. This suggests little to no changes in the general flow and physical conditions prevailing in the aquifer over the 2 years of observations.

4.2. Stable isotopes

On the Vistrenque catchment, all groundwater and surface water samples plot along the Local Meteoric Water Line (LMWL; $\delta^{2}H = 7.6\ \delta^{18}O + 6.4$), defined by Avignon precipitations, collected at 45 km North East from Nîmes (Celle et al., 2000). Despite a slightly lower slope, the LMWL remains close to the Global Meteoric Water Line (GMWL; $\delta^{2}H = 8.13\ \delta^{18}O + 10.8$) (Craig, 1961;

Rozanski et al., 1993), which is shown for comparison (Fig. 2a). This attests that the collected groundwater samples are mainly originated from rainfall infiltration. As $\delta^{18}O$ and $\delta^{2}H$ followed similar trends, $\delta^{2}H$ data will be considered hereinafter, for simplification purposes, since it is the most discriminating parameter of both. For groundwater bodies, $\delta^{2}H$ signature varies between −38‰ and −63‰ for the Vistrenque and Costières samples, and between −42‰ and −47‰ for the karst groundwater samples (Fig. 2b). Stream water is represented by average as well as minimum and maximum values recorded over a hydrological year ($\delta^{2}H_{mean}$ = −55.7‰; $\delta^{2}H_{min}$ = −65.7‰; and $\delta^{2}H_{max}$ = −43.1‰ vs. V-SMOW) approximately 10 km downstream from the head. The imported Rhône River water (n = 6) shows the most depleted signatures, with $\delta^{2}H$ ranging between −66‰ and −77‰ vs. V-SMOW (Fig. 2b). As it is diverted from the Rhône River ($\delta^{2}H$ = −69.3‰ vs. V-SMOW; de Montety et al., 2008), imported water is expected to show depleted signatures compared to local water bodies, owing to the high relief of the Rhône watershed (The Alps, Massif Central, Jura and Vosges mountains). This is often the case for most imported surface water, usually brought by gravity from higher elevation areas (Moran and Hudson, 1990; Williams and Rodoni, 1997).

Annual and winter volume weighted average (VWA) compositions of rainwater are shown for comparison. As the recharge may be predominant in winter, winter VWA is calculated taking into account rainfall events from September to March. The 7 years $\delta^{18}O$ and $\delta^{2}H$ VWA obtained for Nîmes rainwater ($\delta^{2}H$ = −29.9‰ to −38.6‰ vs. V-SMOW (n = 7) (this study and Ladouche et al. (2009)) are very close to those measured at Avignon station over 12 years (Mean $\delta^{2}H$ = −39.5‰ vs. V-SMOW) (IAEA/WMO, 2009). On both Avignon and Nîmes stations, winter VWAs provide more depleted compositions, by approximately 6–8‰, than annual VWA, with a mean $\delta^{2}H$ of −42‰ and −46‰ vs. V-SMOW for Nîmes and Avignon respectively.

Over the 34 boreholes sampled from the Vistrenque aquifer (21 from Table 1S and 13 from Table 2S), only 3 boreholes show an isotopic composition falling in the range of annual VWA rainfall. 26 Vistrenque boreholes, along with 5 Costières boreholes (Table 2S), fall within the range of winter VWA rainfall signature. The remaining 5 Vistrenque boreholes (8, 15, 16, 19, and 29) and 3 Costières boreholes (C1, C3, and C4) are even more depleted than winter VWA rainfall signature, reaching values as low as −61‰ vs. V-SMOW.

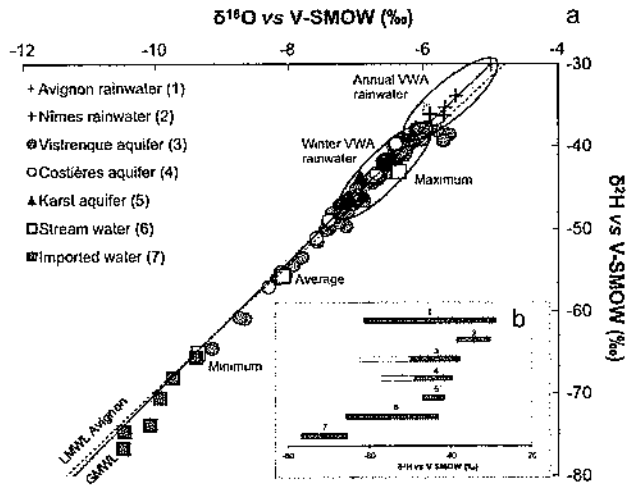

Fig. 2. (a) $\delta^{18}O$ vs. $\delta^{2}H$ (‰ vs. V-SMOW) diagram for all water samples. The GMWL and the LMWL are plotted in straight and in dashed lines respectively; (b) variation of $\delta^{2}H$ in the different water bodies existing in the study site. The numbers above the bars represent water bodies from the legend of (a). The dotted bars represent depleted outliers from the Vistrenque and the Costières GW bodies. The rainwater at Avignon and Nîmes stations are represented by the VWA on 12 and 7 years respectively.

4.3. Major ions and bromides

Major ion analyses, presented in a Piper diagram (Fig. 1S; Supplementary data), show that all considered water bodies in the study area are of Ca–HCO_3 type. Since both the Costières and the Vistrenque aquifers are made of the same alluvial deposits, the Costières groundwater exhibits the same geochemical facies as the bulk of the Vistrenque groundwater.

Within the Ca–HCO_3 Vistrenque groundwater geochemical facies, two minor trends originate from the bulk of the groundwater:

- The first one, toward a Ca–SO_4 type, for groundwater sites located at the South of the aquifer (sites 16, 17, 18, and 21), showing higher proportions in Cl, SO_4, and NO_3.
- The second one, toward a Na–K–HCO_3 type, for 3 groundwater sites located near stream water bodies (sites 5, 6, and 15), following the same trend as stream water, and for 2 sites located in the FPE spreading field (sites 13 and 14). These groundwater samples show, in general, higher proportions of Cl and Na, and in particular, higher proportions of SO_4 (sites 13, 14) and K (sites 5, 6, 15).

Pristine karst water, determined by Maréchal et al. (2005), features very high Ca proportions reaching 95%, while karst samples collected during this study are further enriched in Cl, Na, and K, as is the alluvial groundwater following the Na–K–HCO_3 trend. This Cl, Na and K enrichment, also observed in stream water samples, is generally due to the contribution of sewage effluents (landfills, septic tanks, wastewater treatment plants), specifically rich in these elements, to the surrounding environment (Andersen et al., 2004). In karst samples, it may be explained by the impact of a municipal landfill (highly mineralized suboxic system; Maréchal et al., 2004) upgradient from the boreholes or by the influence of a dense individual septic tanks system in this urbanized area. In streams, the water quality is more likely influenced by direct discharge of wastewater treatment plant (WWTP) effluents (Fig. 1S).

The Cl reference "Cl_{ref}" (Grosbois et al., 2000; Huang and Pang, 2010), corresponding to the Cl input from evapo-concentrated rainwater infiltration to groundwater, is determined by multiplying the Cl concentrations in rainwater, here varying between 0.03 and 0.13 mmol L^{-1} (Ladouche et al., 2009 and this study) by a concentration factor "f", where:

$$f = \text{Rainfall}/(\text{Rainfall} - \text{Evapotranspiration}).$$

The f factor is derived from monthly rainfall and potential evapotranspiration data, on Nîmes–Courbessac weather station, over the last 30 years (http://publitheque.meteo.fr/).

Over that period, the average annual precipitation and evapotranspiration amounts are of 758 mm and 485 mm respectively, and the annual f factor ranges between 1.8 and 8.4, giving a Cl_{ref} varying between 0.05 and 1.1 mmol L^{-1}.

Cl concentrations in the Vistrenque groundwater show significant variations between 0.5 and 3 mmol L^{-1}, corresponding to 3 times the Cl_{ref}. As a first hypothesis, the Vistrenque groundwater samples with Cl concentrations lower than the $Cl_{ref\ max}$ (1.1 mmol L^{-1}) (sites 1–4, 7–12, and 20) may be issued from a direct recharge, as is also the case of the Costières and pristine karst groundwater. The pristine alluvial groundwater is determined on the basis of the Cl_{ref} and the comparison with the Costières groundwater composition. The Vistrenque groundwater samples with Cl concentrations higher than the $Cl_{ref\ max}$, either

located near stream water bodies (sites 5, 6, 15), in areas with intensive agricultural activity (sites 16, 17, 18, and 21) or in the FPE spreading field (sites 13, 14), as well as karst water samples of this study and stream water samples, imply an additional source of Cl in the water bodies such as fertilizers, de-icing streets, septic effluents, or landfills leachates.

The saturation indices (SI) with respect to calcite of the Vistrenque samples, computed with the geochemical code PHREEQC, show that groundwater samples are near equilibrium with respect to calcite (SI = − 0.5 to 0.8).

Na, K, Ca, Br/Cl molar ratios, SO_4, and NO_3 are plotted vs. Cl, in binary diagrams, for all water bodies (Fig. 3a–f). The Br/Cl_{molar} ratios in precipitations ranged between 0.11×10^{-3} and 2.63×10^{-3}, with an average of 1.45×10^{-3}, close to the Mediterranean sea Br/Cl_{molar} ratio (1.57×10^{-3}, de Montety et al., 2008). In groundwater bodies, Br/Cl_{molar} ratios are mostly above the average Br/Cl ratio of rainwater; they vary between 1.13×10^{-3} and 3.44×10^{-3} (Fig. 3b), and tend to decrease with the increase in Cl concentrations. Imported water shows significant variations in Br/Cl ratios, according to the different sampling dates, while

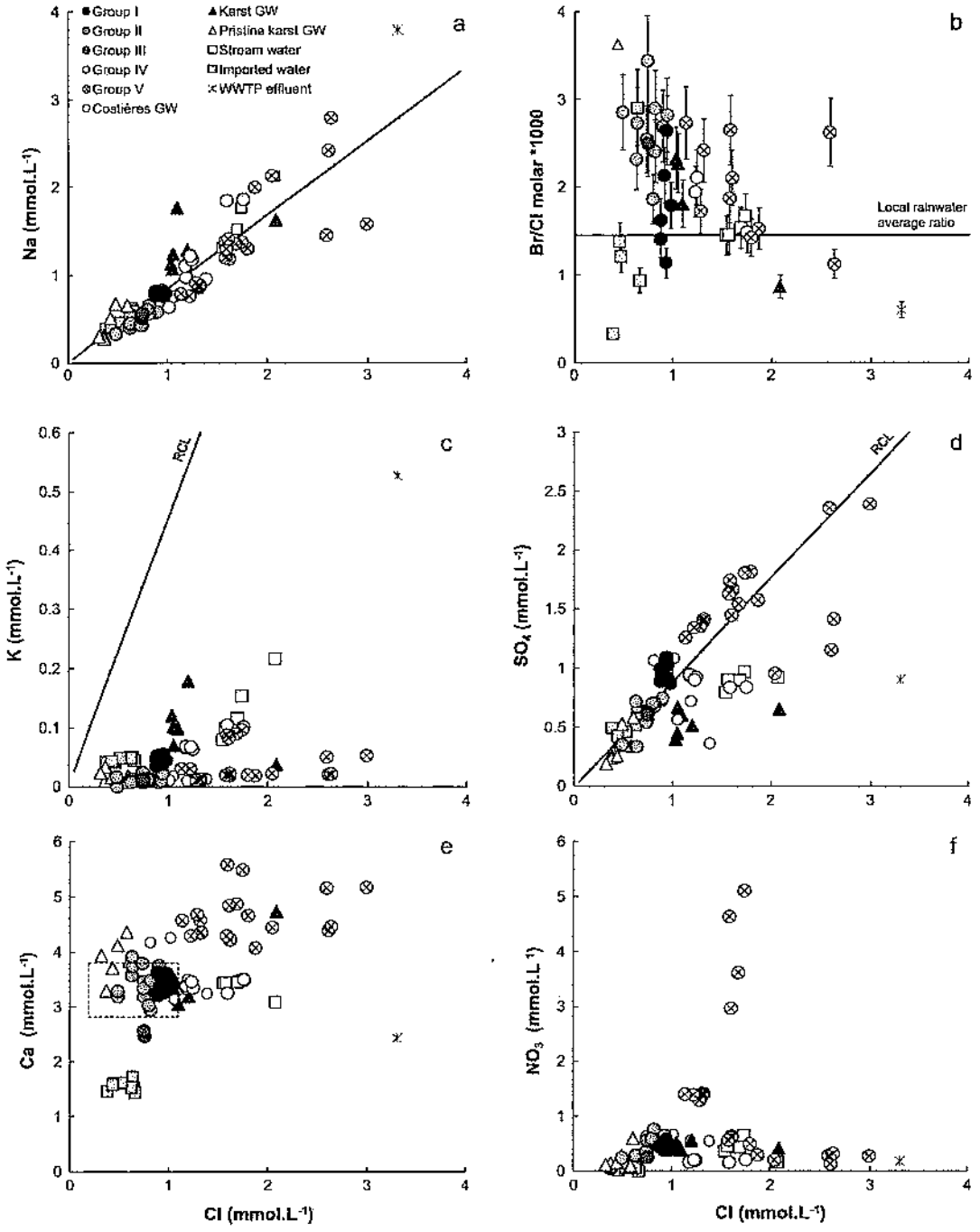

Fig. 3. Na (a), K (c), SO_4 (d), Ca (e), NO_3 (f) concentrations and Br/Cl molar ratios (b) vs. Cl concentrations plots. Groups I–V correspond to the sub-groups of the Vistrenque groundwater (Section 5.1). The straight line represents the rainwater concentration line (RCL). In (e), the dashed box delineates the natural alluvial groundwater signature.

stream water samples, collected over one day, provide a more constant Br/Cl ratio falling between the bulk of the Vistrenque groundwater and the WWTP effluent compositions ($Br/Cl_{molar} = 0.6 \times 10^{-3}$). The WWTP effluent is characterized by high Cl and low Br contents, giving a low Br/Cl ratio, in agreement with literature (Panno et al., 2006; Vengosh and Pankratov, 1998).

Overall, Na, K and SO_4 concentrations increase with Cl concentrations in the Vistrenque groundwater (Fig. 3a, c, and d). Almost all the alluvial groundwater samples from wells located near the karst boundary (sites 2, 4, 10, 11, and 12) show chemical compositions close to that of pristine karst water, clearly evident in the Ca vs. Cl diagram (Fig. 3e). This result matches with the hypothesis of a lateral recharge of the alluvial aquifer by the karst adjacent aquifer (Dorfliger et al., 1999; Fabre, 1988; Michel and François, 1995). At site 19, also located near the karst boundary, Ca contents decreases and groundwater signature falls between the bulk composition of the Vistrenque groundwater and that of imported water in the Ca vs. Cl diagram (Fig. 3e).

The trend of the Vistrenque groundwater at sites 5, 6 and 15 toward stream water composition, as seen with Piper diagram, is confirmed in all binary diagrams (Fig. 3a–f), highlighting the influence of WWTP effluents on these water samples.

Nitrates concentrations are low in most water bodies, remaining below the European drinking water guideline (0.8 mmol L^{-1}). However, sites located in areas with intensive agricultural activity (16, 17 and 18) make exceptions with NO_3 concentrations reaching 5 mmol L^{-1} (Fig. 3f), most likely related to leakage of nutrient rich solutions, used in hydroponic cultures, toward the aquifer (Fiorotto, 2010). In other sites (13, 14), characterized by suboxic conditions (DO = 0.1–2 mg L^{-1}), with an emission of H_2S smelled in the field, NO_3 and SO_4 seems to be biotically reduced. NO_3 may also be reduced at site 21 (DO = 0.3–1.2 mg L^{-1}), due to the confinement of the aquifer.

4.4. Sr isotopes

Among all water bodies, karst groundwater shows the less radiogenic $^{87}Sr/^{86}Sr$ ratios (0.7076–0.7082) and the highest Sr concentrations (6.4–17.6 µmol L^{-1}). In the Sr mixing diagram (Fig. 4),

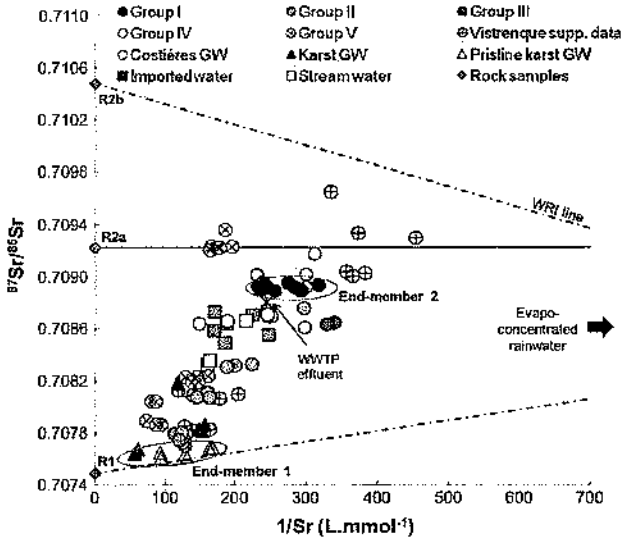

Fig. 4. $^{87}Sr/^{86}Sr$ ratios vs. 1/Sr diagram showing the different water bodies signatures on the Vistrenque catchment. The dashed lines represent the water-rock interaction (WRI) processes between evapo-concentrated rainwater and the rock composition. The Vistrenque supplementary data are from Table 2S (Supplementary data).

pristine karst groundwater samples (Maréchal et al., 2005) plot on a straight line representing the water–rock interaction (WRI) between evapo-concentrated rainwater and the carbonated fraction composition of Hauterivian limestone, R1 ($^{87}Sr/^{86}Sr = 0.7075$; Table 3S) as end-members (Faure, 1986) (Fig. 4). A concentration factor of 4 is considered for rainwater. The karst water in Hauterivian formation seems less radiogenic compared to karst groundwater from Jurassic (Aquilina et al., 2002) and Urgonian/Cretaceous formations (Khaska et al., 2013), on a regional scale. Karst water sampled during this study shows slightly more radiogenic Sr isotopic compositions compared to pristine karst water. This signature is most likely related to anthropogenic wastewater influences evidenced with Cl, Na and K contents in Section 4.3. Indeed, the WWTP effluents, that may also represent septic tanks sewage, show a more radiogenic signature than karst groundwater, implying that anthropogenic Sr may have a more radiogenic signature than pristine karst groundwater.

In contrast, the Costières groundwater samples exhibit relatively high $^{87}Sr/^{88}Sr$ ratios (0.7086–0.7092) and low Sr concentrations (3.2–4.3 µmol L^{-1}) (Fig. 4). This Sr signature is coherent with a WRI process involving a more radiogenic component, most likely clayey rich fraction of the alluvial sediment matrix or the outcropping Plaisancian marls rocks of the aquitard. Leaching experiment with de-ionized water on Plaisancian marls, representing the easily leachable Sr, provides a $^{87}Sr/^{86}Sr$ composition of 0.7092 (R2a; Table 3S), very similar to that of the Costières groundwater, and less radiogenic than the rock total Sr isotopic composition of 0.7105 (R2b) (Medini et al., 2014; Table 3S).

The Vistrenque alluvial groundwater exhibits a large range of $^{87}Sr/^{86}Sr$ compositions, varying from that of the karst system (0.7077) to a more radiogenic composition (0.7096), close to that of the easily leachable Sr (R2a; 0.7092) (Table 3S), with decreasing Sr concentrations (8.8–2.2 µmol L^{-1}) (Fig. 4) and (Fig. 2S; Supplementary data). Both imported and stream water Sr signatures plot in the Vistrenque groundwater group, with Sr isotopic compositions and concentrations on the order of 0.7085 and 5.4 µmol L^{-1} respectively (Fig. 4). Stream water signature is close to that of karst water toward the head and tends toward either the Costières composition or the WWTP compositions, suggesting either a discharge of alluvial groundwater in the stream or an input of Sr from WWTP effluents. The similarity between Sr signatures of imported water and the Vistrenque groundwater is more likely due to the common origin of both Villafranchian and Rhodanien alluvium.

4.5. Pesticides

The frequencies of detection and concentrations of triazines in water samples collected in September 2011 and March 2012 are represented in Fig. 5a and b respectively. Triazines are detected in all the Vistrenque groundwater samples with concentrations varying between 7 and 280 ng L^{-1}. Their frequencies of detection decrease in karst groundwater and stream water, to 40% and 50% respectively. Observed concentrations in these water bodies also decreased to values lower than 15 ng L^{-1}. Triazines were not detected in imported water (2 samples).

5. Discussion

5.1. Source partitioning in the alluvial aquifer

In order to investigate the influence of the different water bodies on the Vistrenque recharge, principal component analyses (PCA) is applied using XLSTAT Software, considering a 95% confidence interval. The PCA is a statistical technique used to reduce

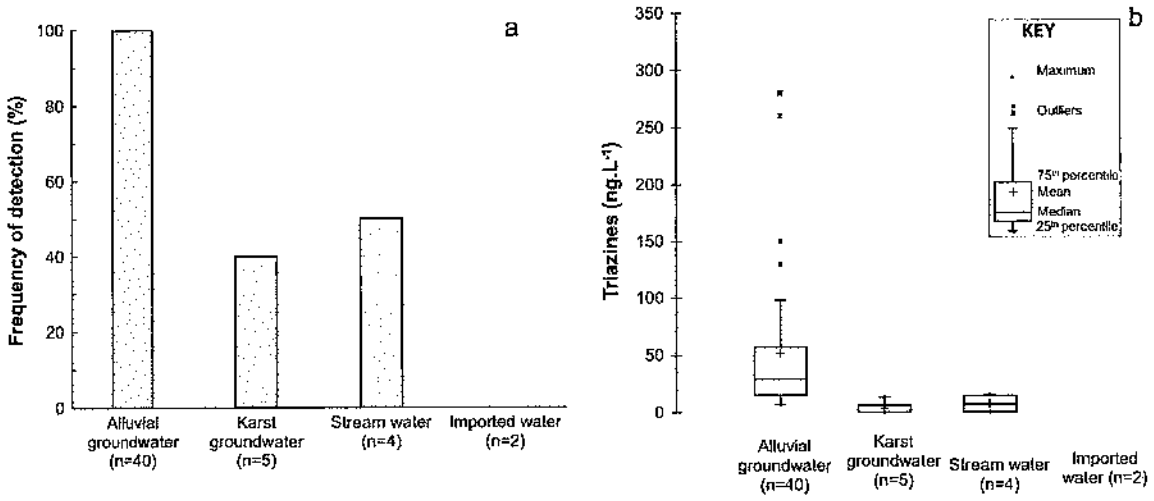

Fig. 5. (a) Frequencies of detection (FD) of triazines in 4 water bodies from the Vistrenque catchment (in imported water, FD = 0); (b) a box plot representing concentrations of triazines in the 4 water bodies. *n* represents the number of observations for each water body.

the number of variables in large data sets to a smaller number of principal components (Wold et al., 1987).

The analysis combines 8 variables (1/Sr, $^{87}Sr/^{86}Sr$, δ^2H, Ca, HCO_3, Na, K, Cl) including both major elements and stable isotopes data, used in the above described multi-tracers approach, for 30 row Vistrenque data samples from Table 1S, as well as for karst water, stream water, imported water, and WWTP effluents (Fig. 6). The 7 years VWA δ^2H composition of Nîmes rainwater was assigned to the pristine karst water in order to include it in the analysis. Only 2 factors are used for interpretation, as they explain 76% of the total variance. The first axis (F1), explaining 41.9% of variability, is mainly defined by Ca, HCO_3, and 1/Sr; which are correlated in a carbonated system. The second axis (F2), explaining 33.9% of variability, is mainly defined by Na and K, which are positively correlated to Cl in sewage signature.

The PCA reveals 3 main groups of variables characterizing 3 different trends, each one correlated to a potential recharge source of the alluvial aquifer.

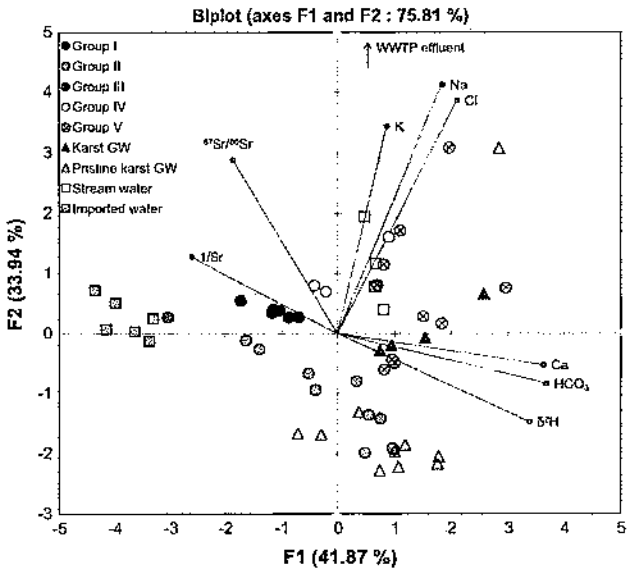

Fig. 6. Variable space computed for 8 elements from 30 Vistrenque groundwater samples.

The samples representing the pristine alluvial groundwater, determined on the basis of Cl_{ref} values and the Costières groundwater hydrochemistry, plot near the origin of F1 and F2 axes (Fig. 6) along 1/Sr and $^{87}Sr/^{86}Sr$ variables, attesting from the fact that they are not influenced by other water sources. The natural average signature of the Villafranchian alluvial groundwater is characterized by δ^2H and $\delta^{18}O$ signatures ranging in the local recharge domain, Cl concentrations ranging between 0.6 and 1 mmol L^{-1}, relatively radiogenic $^{87}Sr/^{86}Sr$ compositions of 0.7088–0.7092 and low Sr concentrations of 3.4 μmol L^{-1}, giving Cl/Sr ratios ranging between 200 and 300.

The first trend groups $^{87}Sr/^{86}Sr$ and 1/Sr in the first quarter of the chart, to which the karst groundwater is inversely correlated. In fact, karst groundwater shows the lowest 1/Sr ratios (150 L $mmol^{-1}$) and the lowest $^{87}Sr/^{86}Sr$ compositions (≈0.7076). The pristine karst groundwater is also characterized by a low mineralization in major elements, except in Ca and HCO_3 (Fig. 3e) (Maréchal et al., 2005). Alluvial groundwater sampled near the karst boundary (sites 4, 10, 11, 12) plots between the pristine alluvial groundwater and the karst groundwater bodies (Fig. 6). The second trend groups Na, K and, Cl variables in the second quarter, to which local stream water is positively correlated following the trend toward the WWTP effluents. The third trend groups Ca, HCO_3 and δ^2H in the fourth quarter, to which imported water is inversely correlated. Only one Vistrenque groundwater sample (site 19) is identified as highly influenced by imported water. Finally, groundwater samples collected from sites influenced by anthropogenic inputs (sites 13, 14, 16, 17, 18) were not considered in the PCA, though they were reported in the graph for comparison. These samples plot on the left half following diverse trends, along the Na, Cl, K, or Ca and HCO_3 factors (Fig. 6), according to the different anthropogenic sources.

Therefore, the alluvial groundwater samples will be classified in 5 groups accordingly:

(i) Group I: representing the pristine alluvial groundwater (sites 7, 8, 9).
(ii) Group II: representing alluvial groundwater influenced by karst groundwater (sites 1, 2, 3, 4, 10, 11, 12, 20).
(iii) Group III: representing alluvial groundwater influenced by imported water (site 19).
(iv) Group IV: representing alluvial groundwater influenced by local stream water (sites 5, 6, 15).

(v) Group V: representing alluvial groundwater influenced by anthropogenic sources (sites 13, 14, 16, 17, 18).

An ascendant hierarchical classification is established to illustrate the relationship between the potential sources and emphasize the relationship between the groups (Fig. 7).

5.2. Origins of water defined using stable isotopes

On the $\delta^{18}O$ vs. $\delta^{2}H$ diagram (Fig. 2a), two contrasting end-members are easily identified: (1) local rainwater showing the most enriched water body in heavy isotopes, and (2) imported water, showing the most depleted signature. Most of the Vistrenque groundwater samples fall in the domain of local recharge, highlighting the infiltration of local rainwater in the aquifer. For the remaining Vistrenque samples, showing a depleted signature with respect to the local recharge, an influence from imported water can be evidenced through a mixing process. This influence may directly occur, through excess irrigation water or canal loss, or indirectly, through depleted surface water infiltration in the aquifer.

The most depleted Vistrenque groundwater sample presents a $\delta^{2}H$ composition of −61‰ vs. V-SMOW on site 19 (group III), located at approximately 600 m downgradient from the imported water canal (Fig. 1a). O and H isotopes are used in mixing models with 2 end-members to further constrain the contribution of imported water to recharge. Assigning the winter VWA rainwater composition as end-member 1 with $\delta^{2}H = -42.5$‰, and the average composition of imported water as end-member 2 with $\delta^{2}H = -72.5$‰, the proportion of imported water on site 19 is estimated at 70% over the 2 years study period. Given this none negligible proportion, this suggests a canal loss at this location.

Imported water may also influence the stream water signature (Fig. 2a), through irrigation, WWTP effluents, and groundwater discharging into the stream.

5.3. Groundwater chemistry

The pristine alluvial groundwater chemistry is classically defined by rainwater infiltration followed by water–rock interaction (WRI) process. As seen in Section 5.1, its hydrochemical signature may be modified by additional sources through mixing processes.

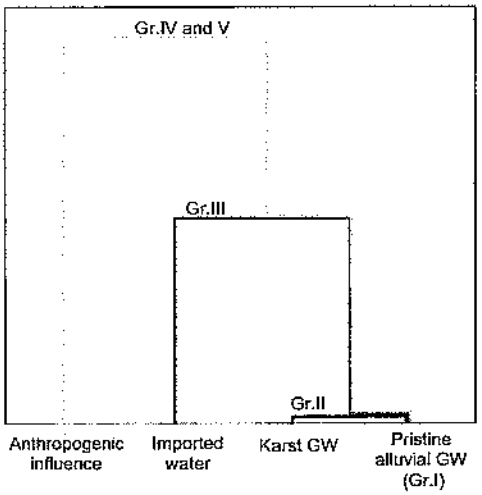

Fig. 7. Hierarchical ascendant classification allowing to define the Vistrenque groundwater groups according to recharge and mineralization origins.

On the one hand, karst water influence may be evidenced by Sr signature. Groundwater sites of group II, located in the confined area of the aquifer (group IIa: 2, 4, 10, 11, 12, with 24, 25, and 27), show a similar Sr composition as the karst groundwater ($^{87}Sr/^{86}Sr = 0.70773–0.70785$; $[Sr] = 6.1–8.8$ µmol L^{-1}), suggesting a high contribution of karst water to the recharge at these sites. Groundwater sites of group II, located in the unconfined area of the alluvial aquifer (group IIb: 1, 3, 20 and 31–34), show an intermediate composition between pure karst water and the Villafranchian alluvial groundwater compositions (Fig. 4), suggesting a mixing process between both water bodies. Such signature could also be issued from a WRI process with alluvial sediments comprising different carbonated fractions. However, on the basis of the $^{87}Sr/^{86}Sr$ vs. Cl/Sr diagram (Fig. 8), samples of group IIb still show an intermediate composition between karst groundwater and pristine alluvial groundwater compositions. Owing to the independent nature of Cl with respect to the calco-carbonic system, the mixing process hypothesis seems to be confirmed for groundwater of group IIb.

Assigning the average pristine alluvial groundwater component as end-member 1 ($^{87}Sr/^{86}Sr = 0.70892$ and $Cl/Sr = 245$), and the average karst groundwater component as end-member 2 ($^{87}Sr/^{86}Sr = 0.70767$ and $Cl/Sr = 62$), the proportion of karst groundwater is estimated using binary mixing models with the 2 end-members (Fig. 8). The karst water proportion reaches 74–100% for groundwater samples of group IIa. This proportion declines to 12–56% for groundwater samples of group IIb.

Hence, the lateral karstic recharge to the Vistrenque groundwater is observed at the scale of the entire North Western border of the aquifer, in varying proportions, and may reach the mid-width of the aquifer. In our study, there was no evidence of contaminated karst water contribution to the recharge of the alluvial aquifer.

On the other hand, mixing processes between pristine alluvial groundwater and stream water, discharging in the aquifer, provide an increase of Cl, Na, and K concentrations (group IV) in alluvial groundwater. On the basis of Cl contents of the average alluvial groundwater and the neighboring stream water, the proportions of stream water infiltrating in the aquifer vary between 20% (sites 5 and 6) and 55% (site 15). When stream water displays more depleted signature in ^{18}O and ^{2}H than local recharge, as is the case of the Vistre stream near site 15, $\delta^{18}O$ and $\delta^{2}H$ may be used to estimate the pro-

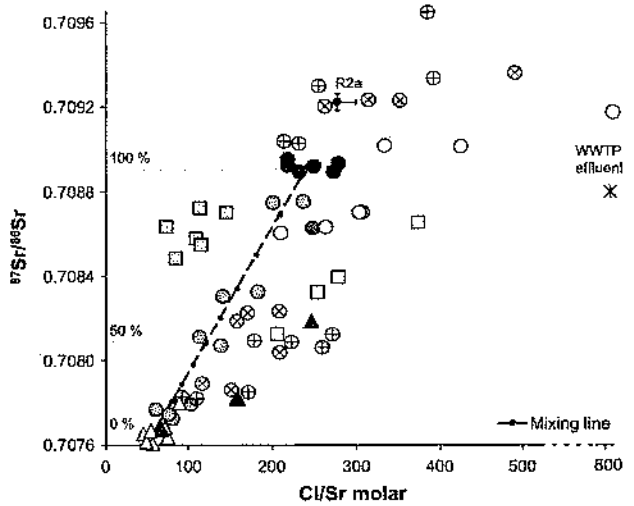

Fig. 8. $^{87}Sr/^{86}Sr$ ratios vs. Cl/Sr molar ratios diagram highlighting a mixing process between pristine karst water and pristine alluvial groundwater in the Vistrenque aquifer, represented by the mixing line. The mixing line is marked every 10% of alluvial groundwater proportion. See Fig. 4 for legend.

portion of stream water infiltrating in the aquifer. The stream water proportion, at site 15, calculated on the basis of ^{18}O and ^{2}H data, reaches 60% which is consistent with that estimated using Cl. Finally, an increase in the alluvial groundwater mineralization may also be provided by agricultural or urban inputs (group V).

5.4. Triazines as groundwater tracer

Despite their prohibition in 2003, triazines are still detected in groundwater bodies due to their persistence in the underground system (Baran et al., 2007; Lapworth and Gooddy, 2006; Loos et al., 2010; Steele et al., 2008; Tesoriero et al., 2007; Vonberg et al., 2014), or in some cases to the persistence of their usage. These compounds, used as selective herbicides in agriculture, can differentiate groundwater originating from different hydrogeosystems with different land uses. Triazines concentrations may vary over the aquifer surface and depth depending on their previous uses and their degradation rates (Baran et al., 2007; Kolpin et al., 1997; Steele et al., 2008; Tesoriero et al., 2007). In this study, the substantial difference in the frequencies of detection and concentrations of triazines among the aquifer types (Fig. 5a and b) is due to the difference in land uses over both the karst area, mainly urbanized or covered with "garrigues" natural type vegetation, and the Vistrenque plain, mainly occupied by agricultural activities. Consequently, the lateral karst recharge induces a dilution in triazines of the Vistrenque groundwater (group IIa) (Fig. 9). Similarly, surface water infiltration, showing low triazines concentrations due to the current interdiction, leads to triazines dilution (group IV) in the alluvial aquifer (Fig. 9).

With respect to imported water influence, dilution of triazines is also expected. Indeed, no triazines were detected in imported water although, 2 samples were only analyzed. The relative absence of triazines is confirmed by analyses of the Rhône River, carried out between 2010 and 2013, showing only 3 occurrences of triazines over that period (http://www.eaufrance.fr/). However, site 19 (group III) showed high triazines concentrations. This may be due to higher triazines concentrations in imported water in the past or to an important local application of triazines which persist in the unsaturated zone reservoir.

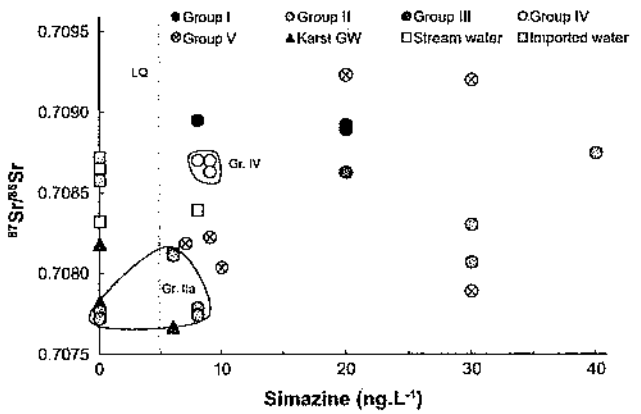

Fig. 9. $^{87}Sr/^{86}Sr$ ratios vs. simazine concentrations diagram showing low simazine concentrations for groundwater samples of groups IIa and IV.

5.5. Vulnerability of groundwater

The quality of the Vistrenque alluvial groundwater is enhanced with respect to triazines and NO_3 contaminations through dilution by adjacent karst groundwater lateral recharge, or by imported Rhône River water infiltration, as these water bodies showed low NO_3 and triazines concentrations (Fig. 10). Yet, the groundwater quality was shown to be locally degraded through mixing processes with infiltrating stream water, which does not only increase the mineralization of groundwater but also may convey microorganisms and emerging organic contaminants such as pharmaceutical compounds and endocrine disruptors. On a larger scale, the degradation of groundwater quality remains dominated by anthropogenic activities on the surface, in particular by agricultural inputs.

Furthermore, in the FPE spreading field, the water chemistry is strongly impacted by the organic matter input leading to suboxic conditions and therefore to biotically driven reduction of NO_3 and SO_4.

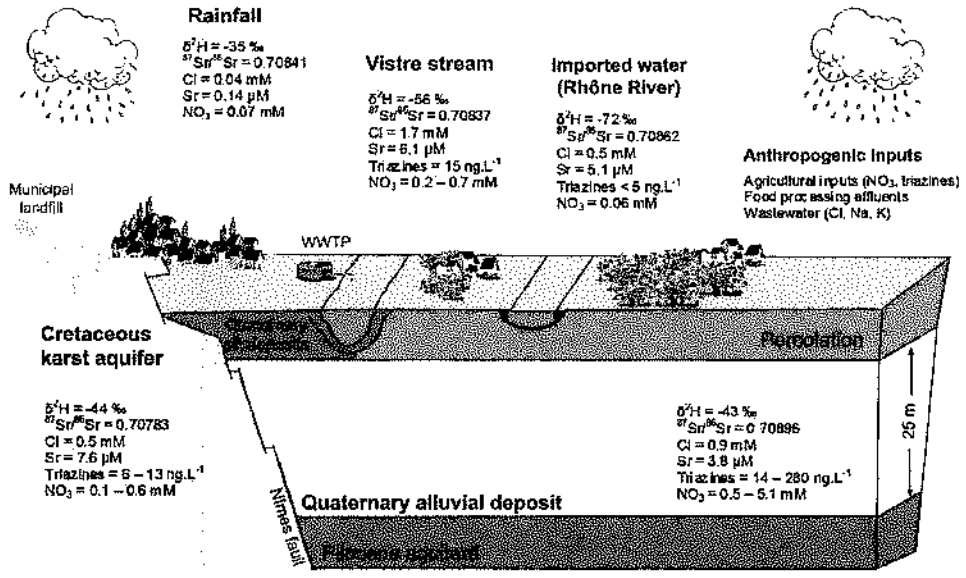

Fig. 10. Conceptual model summarizing the different water bodies on the Vistrenque catchment, their signatures, and the relationships between them.

6. Conclusion

In conclusion, the recharge of the Vistrenque alluvial aquifer is dominated by a direct recharge over the unconfined area as shown by water stable isotopes. Then below the semi-confining layer, on the North Western border, recharge is dominated by the karst adjacent aquifer discharge, which is evidenced by Sr isotopes and confirmed by low contents of pesticides of agricultural usage. Stream water and imported water influences on the Vistrenque alluvial groundwater are locally identified considering $\delta^{18}O$, $\delta^{2}H$ and chemical composition, especially in Cl, Na and K. Karst and imported water may induce dilution of existing NO_3 or anthropogenic pollutions in the aquifer while stream water may increase the major ion concentrations of groundwater through an indirect input from WWTP effluents. Anthropogenic activities turned out to have a non-negligible influence on the quality of the alluvial groundwater highlighting the vulnerability of this shallow aquifer to surface contaminations.

A multi-tracer approach, including traditional elements, isotopes, and micropollutants, proves useful and necessary to answer questions about the groundwater origin and mixing processes occurring in the alluvial aquifer. This method, supported by statistical analyses (PCA), can now be used at a larger scale to identify the origin of groundwater bodies in order to protect the water resource quality.

Acknowledgments

The PhD grant of L. Sassine was supported by the General Council of the Gard Department, the Urban Agglomeration of Nîmes Metropole and the University of Nîmes. A part of this study was also funded by the Joint Venture of the Vistrenque and the Costières Groundwaters. Pr. Aquilina, Dr. Cary and an anonymous reviewer are thanked for their valuable reviews and comments. The stakeholders and landowners are gratefully thanked for giving us the access to the boreholes. We wish to thank Salim Medini for providing the Plaisancian marls samples.

Appendix A. Supplementary material

Supplementary data associated with this article can be found, in the online version, at http://dx.doi.org/10.1016/j.apgeochem.2015.02.001.

References

Aberg, G., 1995. The use of natural strontium isotopes as tracers in environmental studies. Water Air Soil Pollut. 79, 309–322.

Andersen, C.B., Lewis, G.P., Sargent, K.a., 2004. Influence of wastewater treatment effluent on concentrations and fluxes of solutes in the Bush River, South Carolina, during extreme drought conditions. Environ. Geosci. 11, 28–41. http://dx.doi.org/10.1306/eg.10010303017.

Aquilina, L., Ladouche, B., Doerfliger, N., Seidel, J.L., Bakalowicz, M., 2002. Origin, evolution and residence time of saline thermal fluids (Balaruc springs, southern France): implications for fluid transfer across the continental shelf. Chem. Geol. 192, 1–21.

Baran, N., Mouvet, C., Négrel, P., 2007. Hydrodynamic and geochemical constraints on pesticide concentrations in the groundwater of an agricultural catchment (Brévilles, France). Environ. Pollut. 148, 729–738. http://dx.doi.org/10.1016/j.envpol.2007.01.033.

Benedicto, A., Labaume, P., Seguret, M., Séranne, M., 1996. Low-angle crustal ramp and basin geometry in the Gulf of Lion passive margin: Oligocene-Aquitanian Tectonics 15, 1192–1212.

Böhlke, J.K., Horan, M., 2000. Strontium isotope geochemistry of groundwaters and streams affected by agriculture, Locust Grove, MD. Appl. Geochem. 15, 599–609.

Burgeap, Sarl Gren, 2006. Rapport de phase 2: Etude de réhabilitation du Vistre en aval de Nimes. Etude hydrogéologique complémentaire, 41 p.

Cary, L., Casanova, J., Gaaloul, N., Guerrot, C., 2013. Combining boron isotopes and carbamazepine to trace sewage in salinized groundwater: a case study in Cap Bon, Tunisia. Appl. Geochem. 34, 126–139. http://dx.doi.org/10.1016/j.apgeochem.2013.03.004.

Celle, H., Daniel, M., Mudry, J., Blavoux, B., 2000. Signal pluie et traçage par les isotopes stables en Méditerranée occidentale. Exemple de la region avignonnaise (Sud-Est de la France). C. R. Acad. Sci. Géosci. 331, 647–650.

Christophersen, N., Neal, C., Hooper, R.P., Vogt, R.D., Andersen, S., 1990. Modelling streamwater chemistry as a mixture of soilwater end-members: a step towards second-generation acidification models. J. Hydrol. 116, 307–320.

Craig, H., 1961. Isotopic variations in meteoric waters. Science 133, 1702–1703.

De Montety, V., Radakovitch, O., Vallet-Coulomb, C., Blavoux, B., Hermitte, D., Valles, V., 2008. Origin of groundwater salinity and hydrogeochemical processes in a confined coastal aquifer: case of the Rhône delta (Southern France). Appl. Geochem. 23, 2337–2349. http://dx.doi.org/10.1016/j.apgeochem.2008.03.011.

Dogramaci, S.S., Herczeg, A.L., 2002. Strontium and carbon isotope constraints on carbonate-solution interactions and inter-aquifer mixing in groundwaters of the semi-arid Murray Basin, Australia. J. Hydrol. 262, 50–67. http://dx.doi.org/10.1016/S0022-1694(02)00021-5.

Dorfliger, N., Ladouche, B., Desprats, J., Schoen, R., Wittwer, C., 1999. Eaux souterraines et inondations, bassin d'alimentation de la ville de Nîmes. Rapport d'activités 1998. Montpellier, Rapport BRGM – RP 40648.

European Commission, 2000. Directive 2000/60/EC of the European Parliament and of the Council of 23 October 2000 Establishing a Framework for Community Action in the Field of Water Policy. Official Journal of the European Union L 327/1 22/12/2000.

European Commission, 2006. Directive 2006/118/EC of the European Parliament and the Council of 12th of December 2006 on the Protection of Ground Water against Pollution and Deterioration. Official Journal of the European Union L 372/19 27/12/2006.

Fabre, G., 1988. Rapport "préliminaire" N1. L'apport et le rôle des aquifères dans le phénomène d'inondation du 3 octobre 1988 – Rapport ville de Nîmes. Commission hydraulique, CNRS.

Fabre, G., 1997. Le bassin d'alimentation de la fontaine de Nîmes d'après les expériences de traçages. Bul. Soc. et Sc. Nat. Nîmes et Gard 61, 52–57.

Faure, G., 1986. Principles of Isotope Geology. Wiley, New York.

Fiorotto, A., 2010. Etude de protection du captage d'eau potable contre les pollutions diffuses. Commune du Cailar. Rapport final Terra-sol, 103 p.

Fram, M.S., Belitz, K., 2011. Occurrence and concentrations of pharmaceutical compounds in groundwater used for public drinking-water supply in California. Sci. Total Environ. 409, 3409–3417. http://dx.doi.org/10.1016/j.scitotenv.2011.05.053.

Frost, C.D., Toner, R.N., 2004. Strontium isotopic identification of water-rock interaction and ground water mixing. Ground Water 42, 418–432.

Gosselin, D.C., Edwin Harvey, F., Frost, C., Stotler, R., Allen Macfarlane, P., 2004. Strontium isotope geochemistry of groundwater in the central part of the Dakota (Great Plains) aquifer, USA. Appl. Geochem. 19, 359–377. http://dx.doi.org/10.1016/S0883-2927(03)00132-X.

Gourcy, L., Brenot, A., 2011. Multiple environmental tracers for a better understanding of water flux in a wetland area (La Bassée, France). Appl. Geochem. 26, 2147–2158. http://dx.doi.org/10.1016/j.apgeochem.2011.07.012.

Grosbois, C., Négrel, P., Fouillac, C., Grimaud, D., 2000. Dissolved load of the Loire River: chemical and isotopic characterization. Chem. Geol. 170, 179–201. http://dx.doi.org/10.1016/S0009-2541(99)00247-8.

Hooper, R.P., 2001. Applying the scientific method to small catchment studies: a review of the Panola Mountain experience. Hydrol. Process. 15, 2039–2050. http://dx.doi.org/10.1002/hyp.255.

Hooper, R.P., Christophersen, N., Peters, N.E., 1990. Modelling streamwater chemistry as a mixture of soilwater end-members: an application to the Panola mountain catchment, Georgia, USA. J. Hydrol. 116, 321–343.

Huang, T., Pang, Z., 2010. Estimating groundwater recharge following land-use change using chloride mass balance of soil profiles: a case study at Guyuan and Xifeng in the Loess Plateau of China. Hydrogeol. J. 19, 177–186. http://dx.doi.org/10.1007/s10040-010-0643-8.

IAEA/WMO, 2009. Global Network of Isotopes in Precipitation. The GNIP Database. <http://isohis.iaea.org> (WWW Document).

Khaska, M., La Salle, C. Le Gal, Lancelot, J., Asterfeam, Mohamad, A., Verdoux, P., Noret, A., Simler, R., 2013. Origin of groundwater salinity (current seawater vs. saline deep water) in a coastal karst aquifer based on Sr and Cl isotopes. Case study of the La Clape massif (southern France). Appl. Geochem. 37, 212–227. http://dx.doi.org/10.1016/j.apgeochem.2013.07.006.

Kolpin, D.W., Kalkhoff, S.J., Goolsby, D.A., Sneck-Fahrer, D.A., Thurman, M.E., 1997. Occurrence of selected herbicides and herbicide degradation products in Iowa's groundwater 1995. Ground Water 35, 679–688.

Kolpin, D.W., Schnoebelen, D.J., Thurman, M.E., 2004. Degradates provide insight to spatial and temporal trends of herbicides in ground water. Ground Water 42, 601–608.

Ladouche, B., Aquilina, L., Dörfliger, N., 2009. Chemical and isotopic investigation of rainwater in Southern France (1996–2002): potential use as input signal for karst functioning investigation. J. Hydrol. 367, 150–164. http://dx.doi.org/10.1016/j.jhydrol.2009.01.012.

Lapworth, D.J., Gooddy, D.C., 2006. Source and persistence of pesticides in a semi-confined chalk aquifer of southeast England. Environ. Pollut. 144, 1031–1044. http://dx.doi.org/10.1016/j.envpol.2005.12.055.

Lapworth, D.J., Baran, N., Stuart, M.E., Ward, R.S., 2012. Emerging organic contaminants in groundwater: a review of sources, fate and occurrence. Environ. Pollut. 163, 287–303. http://dx.doi.org/10.1016/j.envpol.2011.12.034.

Loos, R., Locoro, G., Comero, S., Contini, S., Schwesig, D., Werres, F., Balsaa, P., Gans, O., Weiss, S., Blaha, L., Bolchi, M., Gawlik, B.M., 2010. Pan-European survey on

the occurrence of selected polar organic persistent pollutants in ground water. Water Res. 44, 4115–4126. http://dx.doi.org/10.1016/j.watres.2010.05.032.
Maréchal, J., Petit, V., Ladouche, B., 2004. Synthèse des connaissances géologiques et hydrogéologiques sur le bassin d'alimentation de la Fontaine de Nîmes. BRGM/RP-53422-FR, 75p.
Maréchal, J., Ladouche, B., Courtois, N., Dörfliger, N., Le Strat, P., Bironne, A., 2005. Modèle conceptuel de la structure et du fonctionnement du système karstique de la Fontaine de Nîmes. BRGM/RP-53827-FR, 187 p.
Maréchal, J., Ladouche, B., Dorfliger, N., 2008. Karst flash flooding in a Mediterranean karst, the example of Fontaine de Nîmes. Eng. Geol. 99, 138–146. http://dx.doi.org/10.1016/j.enggeo.2007.11.013.
Mas-Pla, J., Menció, A., Marsiñach, A., 2012. Basement groundwater as a complementary resource for overexploited stream-connected alluvial aquifers. Water Resour. Manage. 27, 293–308. http://dx.doi.org/10.1007/s11269-012-0186-y.
Medini, S., Janin, M., Techer, I., 2014. Caractérisation isotopique en Sr des produits oléicoles – Application à la traçabilité géographique des huiles d'olive AOP de Nîmes (France). PhD Student Meeting 2014, Aix-Marseille, France.
Ménillet, F., Paloc, H., 1973. Notice explicative, Carte géologique de France (1/50000). Feuille de Nîmes (965), XXIX-42, Orléans, 40p.
Michel, D., François, J.-M., 1995. Etude de l'aquifère calcaire des Garrigues et de ses relations avec l'aquifère villafranchien, Berga Sud, 28 p.
Mohammed, N., Celle-Jeanton, H., Huneau, F., Le Coustumer, P., Lavastre, V., Bertrand, G., Charrier, G., Clauzet, M.L., 2014. Isotopic and geochemical identification of main groundwater supply sources to an alluvial aquifer, the Allier River valley (France). J. Hydrol. 508, 181–196. http://dx.doi.org/10.1016/j.jhydrol.2013.10.051.
Moran, J.E., Hudson, G.B., 1990. Using Groundwater Age and Other Isotopic Signatures to Delineate Groundwater Flow and Stratification. Report of the U.S. Department of Energy by the University of California, Lawrence Livermore, National Laboratory under Contract No. W-7405-ENG-48.
Négrel, P., Petelet-Giraud, E., Widory, D., 2004. Strontium isotope geochemistry of alluvial groundwater: a tracer for groundwater resources characterisation. Hydrol. Earth Syst. Sci. 8, 959–972. http://dx.doi.org/10.5194/hess-8-959-2004.
Osenbrück, K., Gläser, H.-R., Knöller, K., Weise, S.M., Möder, M., Wennrich, R., Schirmer, M., Reinstorf, F., Busch, W., Strauch, G., 2007. Sources and transport of selected organic micropollutants in urban groundwater underlying the city of Halle (Saale), Germany. Water Res. 41, 3259–3270. http://dx.doi.org/10.1016/j.watres.2007.05.014.
Panno, S.V., Hackley, K.C., Hwang, H.H., Greenberg, S.E., Krapac, I.G., Landsberger, S., O'Kelly, D.J., 2006. Characterization and identification of Na-Cl sources in ground water. Ground Water 44, 176–187. http://dx.doi.org/10.1111/j.1745-6584.2005.00127.x.
Penna, D., Stenni, B., Šanda, M., Wrede, S., Bogaard, T.A., Gobbi, A., Borga, M., Fischer, B.M.C., Bonazza, M., Chárová, Z., 2010. On the reproducibility and repeatability of laser absorption spectroscopy measurements for δ^2H and $\delta^{18}O$ isotopic analysis. Hydrol. Earth Syst. Sci. Discuss. 7, 2975–3014. http://dx.doi.org/10.5194/hessd-7-2975-2010.
Pierson-Wickmann, A.-C., Aquilina, L., Weyer, C., Molénat, J., Lischeid, G., 2009. Acidification processes and soil leaching influenced by agricultural practices revealed by strontium isotopic ratios. Geochim. Cosmochim. Acta 73, 4688–4704. http://dx.doi.org/10.1016/j.gca.2009.05.051.
Pin, C., Joannon, S., Bosq, C., Le Fèvre, B., Gauthier, P.-J., 2003. Precise determination of Rb, Sr, Ba, and Pb in geological materials by isotope dilution and ICP-quadrupole mass spectrometry following selective separation of the analytes. J. Anal. At. Spectrom. 18, 135–141. http://dx.doi.org/10.1039/b211832g.
Poul, X., Bayer, F., Buard, C., 1975. Etude hydrogéologique de la Costière – Vistrenque (Gard). Rapport BRGM 75 SGN 220 LRO, 120 p.
Rains, M.C., Mount, J.F., 2002. Origin of shallow ground water in an alluvial aquifer as determined by isotopic and chemical procedures. Ground Water 40, 552–563.
Ray, C., 2002. Riverbank Filtration: Understanding Contaminant Biogeochemistry and Pathogen Removal, first ed. Springer, 253 p.
Rozanski, K., Araguas-Araguas, L., Gonfiantini, R., 1993. Isotopic patterns in modern global precipitation. In: Swart, P.K., Lohmann, K.C., Mckenzie, J., Savin, S. (Eds.), Climate Change in Continental Isotopic Records. American Geophysical Union, Washington, DC. http://dx.doi.org/10.1029/GM078p0001.
Séranne, M., Benedicto, A., Labaum, P., Truffert, C., Pascal, G., 1995. Structural style and evolution of the Gulf of lion Oligo-Miocene rifting: role of the Pyrenean orogeny. Mar. Pet. Geol. 12, 809–820.
SMNVC, 2010. SAGE du Vistre et des nappes Vistrenque et Costières, 240p.
Stalker, J., Kennedy, C., Bowen, G.J., 2010. Determining the spatial influence of imported and local water sources to municipal tap water systems in the southwestern United States using stable isotopes of oxygen and hydrogen. In: AGU Fall Meeting Abstracts.
Steele, G.V., Johnson, H.M., Sandstrom, M.W., Capel, P.D., Barbash, J.E., 2008. Occurrence and fate of pesticides in four contrasting agricultural settings in the United States. J. Environ. Qual. 37, 1116–1132. http://dx.doi.org/10.2134/jeq2007.0166.
Stuart, M., Lapworth, D., Crane, E., Hart, A., 2012. Review of risk from potential emerging contaminants in UK groundwater. Sci. Total Environ. 416, 1–21. http://dx.doi.org/10.1016/j.scitotenv.2011.11.072.
Tesoriero, A.J., Saad, D.A., Burow, K.R., Frick, E.A., Puckett, L.J., Barbash, J.E., 2007. Linking ground-water age and chemistry data along flow paths: implications for trends and transformations of nitrate and pesticides. J. Contam. Hydrol. 94, 139–155. http://dx.doi.org/10.1016/j.jconhyd.2007.05.007.
Thiros, S.A., Manning, A.H., 2004. Quality and Sources of Ground Water used for Public Supply in Salt Lake Valley, Salt Lake County, Utah, 2001, 108 p.
Vengosh, A., Pankratov, I., 1998. Chloride/bromide and chloride/fluoride ratios of domestic sewage effluents and associated contaminated ground water. Ground Water 36, 815–824.
Vitoria, L., Otero, N., Soler, A., Canals, A., 2004. Fertilizer characterization: isotopic data (N, S, O, C, and Sr). Environ. Sci. Technol. 38, 3254–3262.
Voerkelius, S., Lorenz, G.D., Rummel, S., Quétel, C.R., Heiss, G., Baxter, M., Brach-Papa, C., Deters-Itzelsberger, P., Hoelzl, S., Hoogewerff, J., Ponzevera, E., Van Bocxstaele, M., Ueckermann, H., 2010. Strontium isotopic signatures of natural mineral waters, the reference to a simple geological map and its potential for authentication of food. Food Chem. 118, 933–940. http://dx.doi.org/10.1016/j.foodchem.2009.04.125.
Vonberg, D., Vanderborght, J., Cremer, N., Pütz, T., Herbst, M., Vereecken, H., 2014. 20 Years of long-term atrazine monitoring in a shallow aquifer in western Germany. Water Res. 50, 294–306. http://dx.doi.org/10.1016/j.watres.2013.10.032.
Williams, A.E., 1997. Stable isotope tracers: natural and anthropogenic recharge, Orange County, California. J. Hydrol. 201, 230–248. http://dx.doi.org/10.1016/S0022-1694(97)00042-5.
Williams, A.E., Roduni, D.P., 1997. Regional isotope effects and application to hydrologic investigations in southwestern California. Water Resour. Res. 33, 1721–1729.
Wold, S., Esbensen, K., Geladi, P., 1987. Principal component analysis. Chemometr. Intell. Lab. Syst. 2, 37–52. http://dx.doi.org/10.1016/0169-7439(87)80084-9.